

Multi-Level Attention Pooling for Graph Neural Networks: Unifying Graph Representations with Multiple Localities

Takeshi D. Itoh, Takatomi Kubo*, Kazushi Ikeda

Mathematical Informatics Laboratory, Graduate School of Science and Technology, Nara Institute of Science and Technology, 8916-5
Takayama-Cho, Ikoma, Nara 630-0192, Japan

Abstract

Graph neural networks (GNNs) have been widely used to learn vector representation of graph-structured data and achieved better task performance than conventional methods. The foundation of GNNs is the message passing procedure, which propagates the information in a node to its neighbors. Since this procedure proceeds one step per layer, the scope of the information propagation among nodes is small in the early layers, and it expands toward the later layers. The problem here is that the model performances degrade as the number of layers increases. A potential cause is that deep GNN models tend to lose the nodes' local information, which would be essential for good model performances, through many message passing steps. To solve this so-called oversmoothing problem, we propose a multi-level attention pooling (MLAP) architecture. It has an attention pooling layer for each message passing step and computes the final graph representation by unifying the layer-wise graph representations. The MLAP architecture allows models to utilize the structural information of graphs with multiple levels of localities because it preserves layer-wise information before losing them due to oversmoothing. Results of our experiments show that the MLAP architecture improves deeper models' performance in graph classification tasks compared to the baseline architectures. In addition, analyses on the layer-wise graph representations suggest that MLAP has the potential to learn graph representations with improved class discriminability by aggregating information with multiple levels of localities.

Keywords: Graph representation learning (GRL), Graph neural network (GNN), Multi-level attention, Message passing, Oversmoothing

1. Introduction

Graph-structured data are found in many fields. A wide variety of natural and artificial objects can be expressed as a graph, such as molecular structural formula, biochemical reaction pathways, brain connection networks, social networks, the link structure of web pages, and abstract syntax trees of computer programs. Because of this ubiquity, machine learning methods on graphs have been actively studied. Thanks to rich information underlying the structure, graph machine learning techniques have shown remarkable performances in various tasks. For example, the PageRank algorithm (Page et al., 1999) computes the importance of each node in a directed graph based on the number of inbound edges to the node. Shervashidze et al. (2011) used a graph kernel method (Kondor & Lafferty, 2002) to predict chemical molecules' toxicity as a graph classification task. Despite these promising applications, classical machine learning techniques on graphs

require difficult and costly processes for manually designing features or kernel functions.

In contrast to those classical graph machine learning methods using hand-crafted features, recent years have witnessed a surge in graph representation learning (GRL; Hamilton et al., 2017a). A GRL model learns a mapping from a node or a graph to a vector representation. The mapping is trained so that the geometric relationships among embedded representations reflect the similarity of structural information in graphs, *i.e.*, nodes with similar local structures have similar representations (Belkin & Niyogi, 2001; Ahmed et al., 2013). The representation provided by the mapping can then be used as an input feature for task-specific models, such as classifiers or regressors. GRL's *learned* graph features are more flexible than the *hand-crafted* features used in classical graph machine learning methods. However, GRL techniques learn a unique vector for each node without sharing parameters among nodes, leading to a high computational cost and a risk of overfitting. Furthermore, since these techniques learn a specific representation for each node, learned models cannot be applied for prediction on novel graphs or nodes that do not appear in the training phase (Hamilton, 2020, Section 3.4).

*Corresponding author.

Email addresses: itoh.takeshi.ik4@is.naist.jp (Takeshi D. Itoh), takatomi-k@is.naist.jp (Takatomi Kubo), kazushi@is.naist.jp (Kazushi Ikeda)

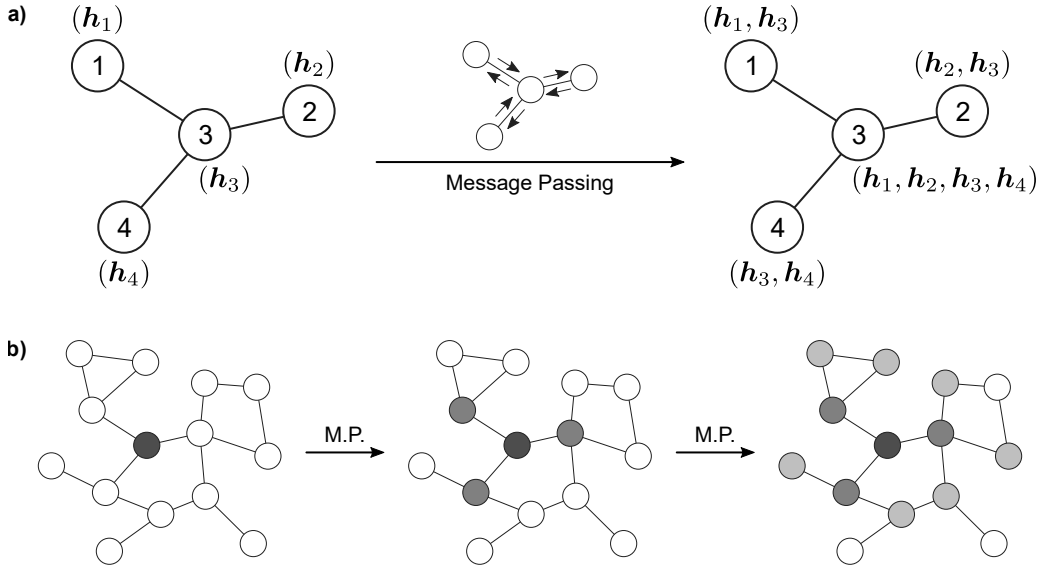


Figure 1: **a)** A schematic illustration of the message passing procedure. i -th node has its original node information, \mathbf{h}_i ($i = 1, \dots, 4$), at the beginning (left). The message passing procedure propagates node information between each pair of connected nodes (center). As a result, each node has its own information and neighbor information after the message passing (right). **b)** The scope of the information propagation changes along the message passing process. The black node in the middle of a graph has only its original node information at the beginning (left). This node obtains information in broader subgraphs through message passing, *i.e.*, dark gray nodes after one message passing step (center) and light gray nodes after two message passing steps (right). *M.P.*: message passing.

More recently, graph neural networks (GNNs) has rapidly emerged as a new framework for GRL (we refer readers to Zhang et al. (2018b) and Wu et al. (2021) for review papers; see Section 2 for related works). Unlike (non-GNN) GRL techniques which learn node-specific representations, GNNs learn how to compute the node representation from the structural information around a node. Hence, GNNs do not suffer from the problem that the computation cost increases linearly to the number of nodes. Furthermore, the learned models generalize to the graphs or nodes which are unknown while training. The foundation of GNNs is the message passing procedure that propagates the information in a node to its neighbor nodes, each of which is directly connected to the source node by an edge (Fig. 1a; see Section 3.1 for detail). Since this procedure proceeds one step per layer, the scope of the information propagation among nodes is small in the early layers, and it expands toward the later layers—*i.e.*, the node representations in the later layers aggregates information from broader subgraphs (Fig. 1b). However, there is an unsolved problem in GNNs that the model performance degrades as the number of layers increases. This is because deep GNN models lose the nodes’ local information, which would be essential for good model performances, through many message passing steps. This phenomenon is known as *oversmoothing* (Li et al., 2018).

In this study, we focus on solving the performance degradation problem for graph-level prediction tasks, such as molecular property classification. Previous studies typically computed the graph representation by a graph pooling layer that collects node representations after the last

message passing layer. Therefore, deeper models cannot utilize nodes’ local information in computing the graph representation because local information is lost through many message passing steps due to oversmoothing. Our approach to solving the problem is aggregating information with multiple levels of localities to compute the graph representation. To this end, we propose a multi-level attention pooling (MLAP) architecture. In short, the MLAP architecture introduces an attention pooling layer (Li et al., 2016) for each message passing step to compute layer-wise graph representations and then unifies them to compute the final graph representation. Our experiments showed performance improvements in deeper GNN models with the MLAP architecture. In addition, analyses on the layer-wise graph representations suggest that MLAP has the potential to learn graph representations with improved class discriminability by aggregating information with multiple levels of localities.

The rest of this paper is organized as follows: Section 2 summarizes related works, Section 3 introduces the proposed MLAP framework, Section 4 describes the experimental setups, Section 5 demonstrates the results, and Section 6 discusses the results and concludes the present study.

2. Related Works

Gori et al. (2005) and Scarselli et al. (2009) first introduced the idea of GNNs, and Bruna et al. (2014) and Defferrard et al. (2016) elaborated the formulation in the graph Fourier domain using spectral filtering. Based on

these earlier works, Kipf & Welling (2017) proposed the graph convolution network, which made a foundation of today’s various GNN models (Duvenaud et al., 2015; Hamilton et al., 2017b; Niepert et al., 2016; Veličković et al., 2018; Xu et al., 2019). Gilmer et al. (2017) summarized these methods as a framework named neural message passing, which computes node representations iteratively by collecting neighbor nodes’ representation using differentiable functions.

In this study, we focus on methods to compute the graph representation from node-wise representations in deeper GNN models. We first summarize the studies on graph pooling methods and then review the recent trends in *deep* GNN studies.

2.1. Graph Pooling Methods

Techniques to learn *graph* representations are usually built upon those to learn *node* representations. A graph-level model first computes the representation for each node in a graph and then collects the node-wise representations into a single graph representation vector. This collection procedure is called a pooling operation. Although there are various pooling methods, they fall into two categories: *global* pooling approach and *hierarchical* pooling approach.

The *Global* pooling approach collects all of the node representations in a single computation. The simplest example of the global pooling method is sum pooling, which merely computes the sum of all node representations. Duvenaud et al. (2015) introduced sum pooling to learn embedded representations of molecules from a graph where each node represents an atom. Likewise, one can compute an average or take the maximum elements as a pooling method. Li et al. (2016) introduced attention pooling, which computes a weighted sum of node representations based on a softmax attention mechanism (Bahdanau et al., 2015). Vinyals et al. (2016) proposed set2set by extending the sequence to sequence (seq2seq) approach for a set without ordering. Zhang et al. (2018a) introduced the SortPooling, which sorts the node representations regarding their topological features and applies one-dimensional convolution. These global pooling methods are simple and computationally lightweight, but they cannot make use of the structural information of graphs in the pooling operation.

In contrast, *hierarchical* pooling methods segment the entire graph into a set of subgraphs hierarchically and compute the representations of subgraphs iteratively. Bruna et al. (2014) introduced the idea of hierarchical pooling, or graph coarsening, based on hierarchical agglomerative clustering. Although some early works like Defferrard et al. (2016) also applied similar approaches, but such clustering-based hierarchical pooling requires the clustering algorithm to be deterministic—that is, the hierarchy of subgraphs is fixed throughout the training. To overcome this limitation, Ying et al. (2018) proposed DiffPool, which learns

the subgraph hierarchy itself along with the message passing functions. They proposed to use a neural network to estimate which subgraph a node should belong to in the next layer. Gao & Ji (2019) extended U-Net (Ronneberger et al., 2015) for graph structure to propose graph U-Nets. Original U-Net introduced down-sampling and up-sampling procedures for semantic image segmentation tasks. Based on the U-Net, graph U-Nets is composed of a gPool network to shrink the graph size hierarchically and a gUnpool network to restore the original graph structure. Cangea et al. (2018) applied gPool to compute graph representations in graph classification tasks. Also, Lee et al. (2019) employed a self-attention mechanism to define a hierarchy of subgraph structures. However, these hierarchical pooling methods are complicated and often difficult to train.

2.2. Oversmoothing in Deep Graph Neural Networks

Kipf & Welling (2017) first reported that deep GNN models with many message passing layers performed worse than shallower models. Li et al. (2018) investigated this phenomenon and found that deep GNN models converged to an equilibrium point wherein connected nodes have similar representations. Since the nodes with similar representations are indistinguishable from each other, such convergence degrades the performance in node-level prediction tasks. This problem is called *oversmoothing*. In graph-level prediction tasks, oversmoothing occurs independently for each graph. Oversmoothing per graph damages GNN models’ expressivity and results in performance degradation (Huang et al., 2020).

Recent studies have focused on residual connections and normalization methods to solve the oversmoothing problem and train deeper GNN models successfully. Residual connections, or ResNet architecture, were first introduced to convolutional neural networks for computer vision tasks, achieving a state-of-the-art performance (He et al., 2016). Kipf & Welling (2017) applied the residual connections in the graph convolutional network and reported that residual connections mitigated the performance degradation in deeper models. Later, Li et al. (2019), Zhang & Meng (2019), and Chen et al. (2020) applied similar residual architectures on GNNs and showed performance improvement. On the other hand, normalization in deep learning gained attention by the success of early works such as BatchNorm (Ioffe & Szegedy, 2015) and LayerNorm Ba et al. (2016). These techniques normalize the tensors along a particular axis. In GNNs, one can define the normalization axis using a graph-specific property. For example, PairNorm (Zhao & Akoglu, 2020) normalizes node representations so that distances between two connected node representation vectors are constant. Cai et al. (2020) proposed GraphNorm to normalize node representations across the whole graph while keeping the structural information for each graph, unlike a previous method (Ulyanov et al., 2016).

Jumping knowledge (JK) network (Xu et al., 2018) is another technique to train deeper GNN models successfully. It is motivated by a similar idea to ours: GNNs should be capable of aggregating information in multiple levels of localities. However, their method computes the final *node* representations by aggregating intermediate node representations in each layer. For graph-level prediction tasks, a pooling layer computes graph representations by collecting these final node representations. JK network improved *node*-level classification task performance, but we consider that aggregating intermediate node representations before pooling is not desirable for *graph*-level tasks because a model cannot preserve the information in multiple levels of localities independently.

3. Methods

This study aims to mitigate the performance degradation problem in deep GNN models for graph-level prediction tasks. To this end, we propose the MLAP architecture to solve the problem, which aggregates graph representation in multiple levels of localities. In this section, we first summarize the fundamentals of GNNs, particularly the message passing procedure, and then introduce the MLAP architecture.

3.1. Preliminaries: Graph Neural Networks

Let $G = (\mathcal{N}, \mathcal{E})$ be a graph, where \mathcal{N} is a set of nodes and \mathcal{E} is a set of edges. $n \in \mathcal{N}$ denotes a node and $e_{n_{\text{src}}, n_{\text{dst}}} \in \mathcal{E}$ denotes a directed edge from a source node n_{src} to a destination node n_{dst} . A graph is characterized by at least either of its node features or edge features, or both of them. If a graph has node features, each node n has a node feature vector \mathbf{p}_n . Similarly, if a graph has edge features, each edge $e_{n_{\text{src}}, n_{\text{dst}}}$ has an edge feature vector $\mathbf{q}_{n_{\text{src}}, n_{\text{dst}}}$.

There are three types of tasks commonly studied for GNNs: graph-level prediction, node-level prediction, and edge-level prediction. In this study, we focus on the graph-level prediction tasks, that is, given a set of graph $\mathcal{G} = \{G_1, \dots, G_{|\mathcal{G}|}\}$ and their labels $\mathcal{Y} = \{y_1, \dots, y_{|\mathcal{G}|}\}$, we want to learn a graph representation vector \mathbf{h}_G used for predicting the graph label $y_G = g(\mathbf{h}_G)$, where g is a predictor function.

Suppose we have a GNN with L layers. Each layer in a GNN propagates the node representation \mathbf{h}_n along the edges (*message passing*). Let $\mathbf{h}_n^{(l)} \in \mathbb{R}^d$ be the representation of n after the message passing by the l -th layer, where d is the dimension of the vector representations. In general, the propagation by the l -th layer first computes the *message* $\mathbf{m}_n^{(l)}$ for each node n from its neighbor nodes $\text{NBR}(n)$, as in

$$\mathbf{m}_n^{(l)} = f_{\text{col}}^{(l)} \left(\left\{ f_{\text{msg}}^{(l)} \left(\mathbf{h}_{n'}^{(l-1)}, \mathbf{q}_{n', n} \right) \mid n' \in \text{NBR}(n) \right\} \right), \quad (1)$$

where $f_{\text{msg}}^{(l)}$ is a message function to compute the message for each neighbor node from the neighbor representation and the feature of the connecting edge, and $f_{\text{col}}^{(l)}$ is a function to collect the neighbor node-wise messages. Then, the layer *updates* the node representation $\mathbf{h}_n^{(l)}$ as

$$\mathbf{h}_n^{(l)} = f_{\text{upd}}^{(l)} \left(\mathbf{m}_n^{(l)}, \mathbf{h}_n^{(l-1)} \right), \quad (2)$$

where $f_{\text{upd}}^{(l)}$ is an update function.

After L steps of message passing, a graph pooling layer computes a graph representation vector \mathbf{h}_G from the final node representations $\mathbf{h}_n^{(L)}$ for each $n \in \mathcal{N}$, as in

$$\mathbf{h}_G = \text{Pool} \left(\left\{ \mathbf{h}_n^{(L)} \mid n \in \mathcal{N} \right\} \right). \quad (3)$$

3.2. Multi-Level Attentional Pooling

Graph-level prediction tasks require the models to utilize both local information in nodes and global information as the entire graphs for good performances. However, typical GNN implementations first execute the message passing among nodes for a certain number of steps L and then pool the node representations into a graph representation, as shown in Eq. (3) (Fig. 2a). This formulation damages GNN models' expressivity because it can only use the information in a fixed locality to compute the graph representation.

To fix this problem, we introduce a novel GNN architecture named multi-level attentional pooling (MLAP; Fig. 2c). In the MLAP architecture, each message passing layer has a dedicated pooling layer to compute layer-wise graph representations, as in

$$\mathbf{h}_G^{(l)} = \text{Pool}^{(l)} \left(\left\{ \mathbf{h}_n^{(l)} \mid n \in \mathcal{N} \right\} \right) \quad \forall l \in \{0, \dots, L\}. \quad (4)$$

Here, we used the attention pooling (Li et al., 2016) as the pooling layer. Thus,

$$\mathbf{h}_G^{(l)} = \sum_{n \in \mathcal{N}} \text{softmax} \left(f_{\text{gate}}(\mathbf{h}_n^{(l)}) \right) \mathbf{h}_n^{(l)} \quad (5)$$

$$= \sum_{n \in \mathcal{N}} \frac{\exp \left(f_{\text{gate}}(\mathbf{h}_n^{(l)}) \right)}{\sum_{n' \in \mathcal{N}} \exp \left(f_{\text{gate}}(\mathbf{h}_{n'}^{(l)}) \right)} \mathbf{h}_n^{(l)}, \quad (6)$$

where f_{gate} is a function used for computing the attention score. We used a two-layer neural network.

Then, an aggregation function computes the final graph representation by unifying the layer-wise representations as following:

$$\mathbf{h}_G = f_{\text{agg}} \left(\left\{ \mathbf{h}_G^{(l)} \mid l \in \{0, \dots, L\} \right\} \right), \quad (7)$$

where f_{agg} is an aggregation function. One can use an arbitrary function for f_{agg} . In the present study, we tested two types of the aggregation function: *sum* and *weighted*.

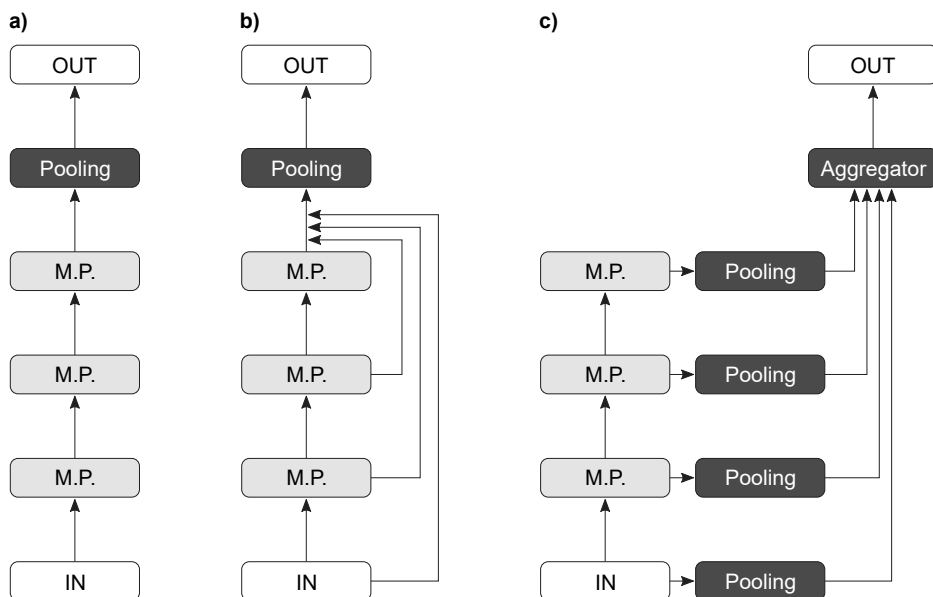


Figure 2: **a)** A naive GNN architecture. A pooling layer computes the graph representation from the node representations after the last message passing. **b)** The jumping knowledge network architecture. A pooling layer computes the graph representation after taking the sum of the layer-wise node representations. **c)** Proposed multi-level attentional pooling (MLAP) architecture. There is a dedicated pooling layer for each message passing layer. The aggregator computes the graph representation from the layer-wise graph representations. *M.P.*: message passing.

3.2.1. sum

One of the simplest ways to aggregate the layer-wise graph representations is to take the sum of them, as in

$$\mathbf{h}_G = \sum_{l=0}^L \mathbf{h}_G^{(l)}. \quad (8)$$

This formulation expresses an assumption that the representation in each layer is equally important in computing the final graph representation.

3.2.2. Weighted

Each layer-wise representation might have different importance depending on the layer index. If this is the case, taking a weighted sum would be adequate to learn such importance of layers, as in

$$\mathbf{h}_G = \sum_{l=0}^L w^{(l)} \mathbf{h}_G^{(l)}, \quad (9)$$

where $\{w^{(l)} \mid l \in \{0, \dots, L\}\}$ is a trainable weight vector.

4. Experiments

4.1. Datasets

We used two datasets from the graph property prediction collection in the open graph benchmark (OGB; Hu et al., 2020) for testing the proposed methods. For both datasets, we followed the standard dataset splitting procedure provided by the OGB.

4.1.1. ogbg-molhiv

The ogbg-molhiv is a dataset for a molecular property prediction task, originally introduced in Wu et al. (2018). Each graph in this dataset represents a molecule. Each node in a graph represents an atom and has a nine-dimensional discrete-valued feature containing the atomic number and other atomic properties. Each edge represents a chemical bond between two atoms and has a three-dimensional discrete-valued feature containing the bond type and other properties. This dataset has a relatively small sample size (41,127 graphs in total), with 25.5 nodes and 27.5 edges per graph on average. The task is a binary classification to identify whether a molecule inhibits the human immunodeficiency virus (HIV) from replication. Model performance is evaluated by the area under the curve value of the radar operator characteristics curve (ROC-AUC).

4.1.2. ogbg-ppa

The ogbg-ppa dataset contains a set of subgraphs extracted from the protein-protein association network of species in 37 taxonomic groups, originally introduced in Szklarczyk et al. (2018). Each node in a graph represents a protein without node features. Each edge represents an association between two proteins and has a seven-dimensional real-valued feature describing the biological meanings of the association. This dataset has a medium sample size (158,100 graphs in total), with 243.4 nodes and 2266.1 edges per graph on average. The task is a classification to identify from which taxonomic group among 37 classes an association graph comes. The performance of a

model is evaluated by the overall classification accuracy.

4.2. Model Configurations

We used the graph isomorphism network (GIN; Xu et al., 2019) as the message passing layer¹ following the OGB’s reference implementation shown in Hu et al. (2020), *i.e.*, in Eqs. (1) and (2),

$$\mathbf{m}_n^{(l)} = \sum_{n' \in \text{NBR}(n)} \text{ReLU} \left(\mathbf{h}_{n'}^{(l-1)} + f_{\text{edge}}^{(l)}(\mathbf{q}_{n',n}) \right), \quad (10)$$

$$\mathbf{h}_n^{(l)} = f_{\text{NN}}^{(l)} \left((1 + \epsilon^{(l)}) \cdot \mathbf{h}_n^{(l-1)} + \mathbf{m}_n^{(l)} \right), \quad (11)$$

where $f_{\text{edge}}^{(l)}$ is a trainable function to encode edge features into a vector, $f_{\text{NN}}^{(l)}$ is a two-layer neural network for transforming node representations, and $\epsilon^{(l)}$ is a trainable scalar weight modifier.

We varied the number of GIN layers L from 1 to 10 to investigate the effect of depth in model performance. We fixed the node representation dimension d to 200. Each GIN layer is followed by GraphNorm (Cai et al., 2020). After the normalization, we added a dropout layer with a dropout ratio of 0.5. We optimized the model using the Adam optimizer (Kingma & Ba, 2015) for 50 epochs. In addition to these configurations, there are dataset-specific settings detailed below.

4.2.1. ogbg-molhiv

We used the OGB’s atom encoder for computing the initial node representation $\mathbf{h}_n^{(0)}$ from the nine-dimensional node feature. We also used the OGB’s bond encoder as $f_{\text{edge}}^{(l)}$ in Eq. (10), which takes the three-dimensional edge feature as its input.

After computing the graph representation \mathbf{h}_G by Eq. (8) or Eq. (9), a linear transformation layer followed by a sigmoid function computes the probability with which each graph belongs to the *positive* class, as in

$$P(\text{positive}|G) = \sigma(\mathbf{w}_{\text{prob}} \cdot \mathbf{h}_G), \quad (12)$$

where σ is a sigmoid function and \mathbf{w}_{prob} is a trainable row vector with the same dimension d as the graph representation vectors.

The models were trained against a binary cross-entropy loss function. The initial learning rate was set to 10^{-4} and decayed by $\times 0.5$ for every 15 epochs. The batch size was set to 20 to avoid overfitting to a small dataset.

4.2.2. ogbg-ppa

We set $\mathbf{h}_n^{(0)} = \mathbf{0}$ because this dataset does not have node features. We used a two-layer neural network as $f_{\text{edge}}^{(l)}$ to embed the edge feature.

Besides GNN, each model learned an embedded class representation matrix $\mathbf{E} \in \mathbb{R}^{37 \times d}$. The probability with which a graph belongs to the class c is computed by a softmax function:

$$P(c|G) = \text{softmax}(\mathbf{E}_c \cdot \mathbf{h}_G) = \frac{\mathbf{E}_c \cdot \mathbf{h}_G}{\sum_{c'=1}^{37} \mathbf{E}_{c'} \cdot \mathbf{h}_G}, \quad (13)$$

where \mathbf{E}_c is the c -th row vector of \mathbf{E} .

The models were trained against a cross-entropy loss function. The initial learning rate was set to 10^{-3} and decayed by $\times 0.2$ for every 15 epochs. The batch size was 50.

4.3. Performance Evaluation

We compared the performance of GNN models with our MLAP framework (Fig. 2c) to two baseline models. One is a naive GNN model that simply stacks GIN layers, wherein the representation of a graph is computed by pooling the node representations after the last message passing (Fig. 2a), as in

$$\mathbf{h}_G = \text{Pool} \left(\left\{ \mathbf{h}_n^{(L)} \mid n \in \mathcal{N} \right\} \right). \quad (14)$$

The other is the JK architecture (Xu et al., 2018), wherein the graph representation is computed from the sum of the intermediate node representations (Fig. 2b; Xu et al., 2019).

$$\mathbf{h}_G = \text{Pool} \left(\left\{ \sum_{l=0}^L \mathbf{h}_n^{(l)} \mid n \in \mathcal{N} \right\} \right). \quad (15)$$

For each of four architectures (*naive*, *JK*, *MLAP-sum*, *MLAP-weighted*), we trained models with varying depth (1–10). We trained six models independently by varying the random seed value from 0 to 5. The performance of an architecture with a certain depth is evaluated by the median of six trained models.

4.4. Analyses on Layer-Wise Representations

We analyzed the layer-wise graph representations to investigate the effectiveness of the MLAP architecture. First, we computed the layer-wise graph representations and the final graph representation after MLAP aggregation for each graph in the training set. We conducted two different analyses on these embedded representations.

4.4.1. t-SNE Visualization

We visualized the distribution of those representations in a two-dimensional space using t-SNE (van der Maaten & Hinton, 2008). The t-SNE hyperparameters were as follows: the learning rate was 50, the number of iteration was 3000, and the perplexity was 20.

¹Note that the MLAP architecture is applicable to any GNN models independent of the type of message passing layers.

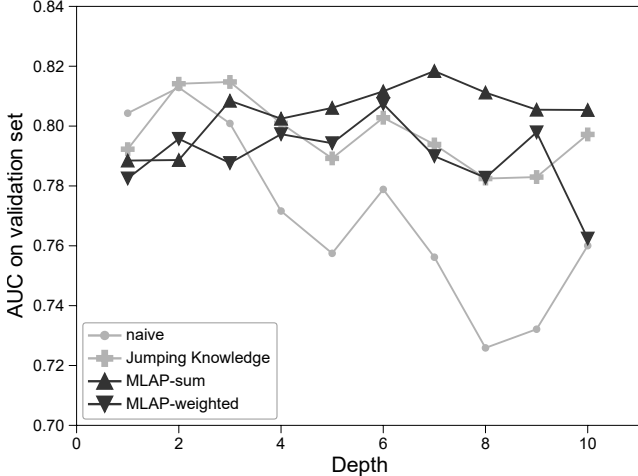


Figure 3: The task performances in ogbg-molhiv experiments for each architecture and depth.

4.4.2. Training Layer-Wise Classifiers

We trained layer-wise classifiers to evaluate the “goodness” of the layer-wise representations quantitatively. We followed the classifier implementations in Eqs. (12) and (13), but the graph representation terms \mathbf{h}_G in those equations were replaced by the pre-computed layer-wise representations $\mathbf{h}_G^{(l)}$. These classifiers were trained on the representations of the training set. The classification performances were tested against the representations of the validation set. The classifiers were optimized by the Adam optimizer (Kingma & Ba, 2015) for 30 epochs with setting the learning rate to 10^{-3} .

5. Results

5.1. Model Performances

5.1.1. ogbg-molhiv

Fig. 3 shows the performances of the model architectures for each network depth evaluated on the validation set in the ogbg-molhiv dataset. Our MLAP architecture using the *sum* aggregator achieved the peak performance (AUC = 0.8184) with $L = 7$. Conversely, the baseline models had their performance peaks in shallower models. The *naive* architecture’s best validation AUC score was 0.8129 when $L = 2$, and that of *JK* architecture was 0.8148 when $L = 3$. The *MLAP-weight* architecture did not improve the model performance.

5.1.2. ogbg-ppa

Fig. 4 shows the performances of models evaluated on the validation set in the ogbg-ppa dataset. For all the architectures, setting $L = 1$ leads to the best performance within each architecture. Although there were no performance improvements by making the model deeper, the *MLAP-sum* architecture showed the smallest performance degradation when the number of layers increased.

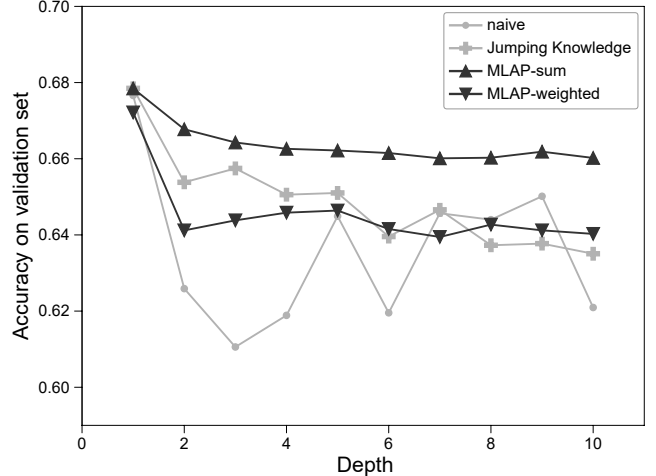


Figure 4: The task performances in ogbg-ppa experiments for each architecture and depth.

5.2. Analyses on Layer-Wise Representations

5.2.1. ogbg-molhiv

We used a seven-layer MLAP-sum model trained with the ogbg-molhiv dataset, whose validation AUC score was 0.8249, for these analyses.

Fig. 5 shows the t-SNE visualization results, where each gray dot represents a *negative* sample, while each black dot represents a *positive* sample. For input graphs ($l = 0$), the positive samples distribute randomly over the manifold. After one message passing step ($l = 1$), a certain proportion of positive samples gather (top-left area in the $l = 1$ panel). Through $l = 2$ to $l = 7$, the localization of positive samples gradually gets weaker. However, computing the sum of all of the layer-wise representations by the MLAP aggregator produces a more localized sample distribution than any representations in the intermediate layers.

The analysis using the layer-wise classifiers supports the intuition obtained from the t-SNE visualization. Fig. 6 shows the training and validation AUC scores for each layer-wise classifier. The best validation score among the intermediate layers (0.7479) was marked at $l = 2$, but the score after MLAP aggregation is better than any intermediate layers (0.8007).

5.2.2. ogbg-ppa

We used a seven-layer MLAP-sum model for these analyses to compare to the model behavior in the ogbg-molhiv task, because analyses using the best performing model with only one layer are useless.

Fig. 7 shows the t-SNE visualization results, wherein dots in different colors indicate samples in different classes. Since the graphs in the ogbg-ppa dataset do not have initial node features \mathbf{p}_n , the t-SNE visualization is not applicable for $l = 0$. Similar to the ogbg-molhiv case, the representations in $l = 1$ showed the best localization of samples in each class. However, unlike ogbg-molhiv, such

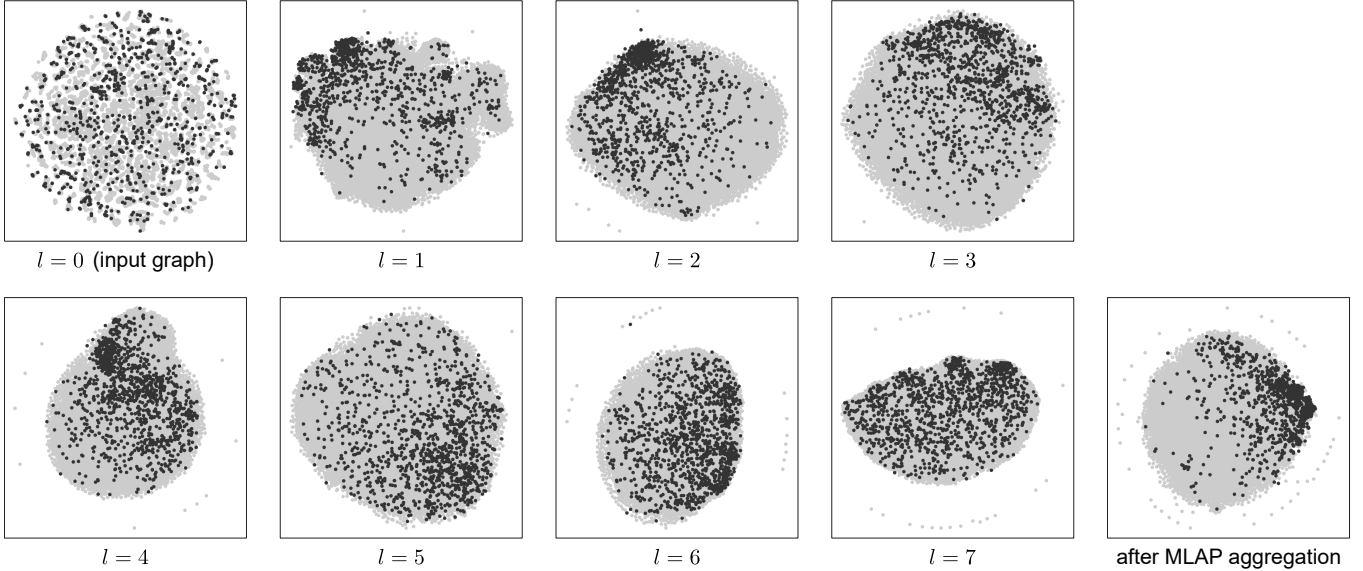


Figure 5: The layer-wise graph representations for ogbg-molhiv graphs. They are visualized in two-dimensional spaces using t-SNE. Each gray dot represents a *negative* sample, while each black dot represents a *positive* sample.

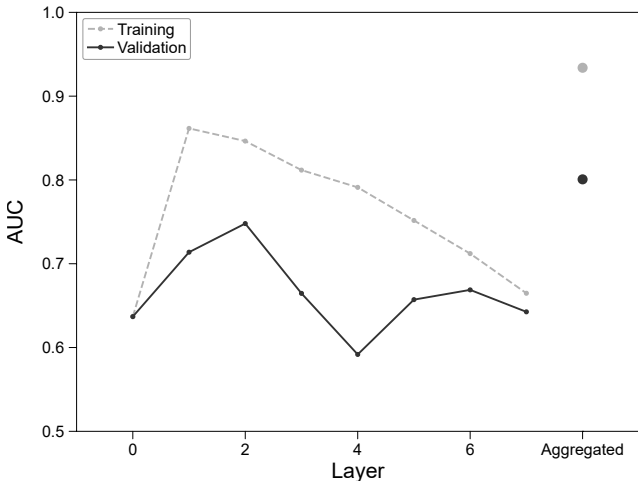


Figure 6: The classification performances of the layer-wise representations computed for ogbg-molhiv graphs. The “Aggregated” in the horizontal axis indicates the classifier’s performance trained with the graph representations after MLAP aggregation.

localization rapidly disappeared after a few message passing steps. The class localization appears again in the representations after MLAP aggregation, but it is not better than the localization seen in $l = 1$.

The layer-wise classifier analysis also showed similar results (Fig. 8). The representations in $l = 1$ achieved the best validation score (0.6285). It was better than the score of the representations after MLAP aggregation (0.6265).

6. Discussion

In this study, we proposed the MLAP architecture for GNNs, which introduces layer-wise graph pooling layer

and computes the final graph representation by unifying the layer-wise graph representations. Experiments showed that our MLAP framework, which can utilize the structural information of graphs with multiple levels of localities, improved deeper GNN models’ performance. The performances of the baseline architectures degraded as the number of layers increased. For the *naive* architecture, this is because the deep *naive* model lost the local structural information through many message passing steps due to oversmoothing. Since the *naive* architecture only uses the node representation after the last message passing step to compute the graph representation, oversmoothing is critical to the model performance. On the other hand, the difference in performance between the *MLAP-sum* and the *JK* would be because of the operation order between the graph pooling and the information aggregation from multiple levels of localities. The *MLAP-sum* computes the graph representations by $\sum_l \text{Pool}^{(l)}(\mathbf{h}_n^{(l)})$, whereas the *JK* computes them by $\text{Pool}(\sum_l \mathbf{h}_n^{(l)})$. Since the *JK* takes sums of node representations in multiple levels of localities *before* the pooling, it might be difficult for the attention mechanism to learn which node to focus on. In contrast, the *MLAP-sum* architecture can tune the attention on nodes specifically in each information locality because it preserves the representations in each locality independently. Also, the performances of *MLAP-weighted* architecture were worse than *MLAP-sum*. This might be caused by instability in training GNN parameters for computing node representations and weight parameters for layers simultaneously.

The analyses on the layer-wise graph representations showed that early layers’ representations had a good discriminability among classes. In contrast, the discriminabil-

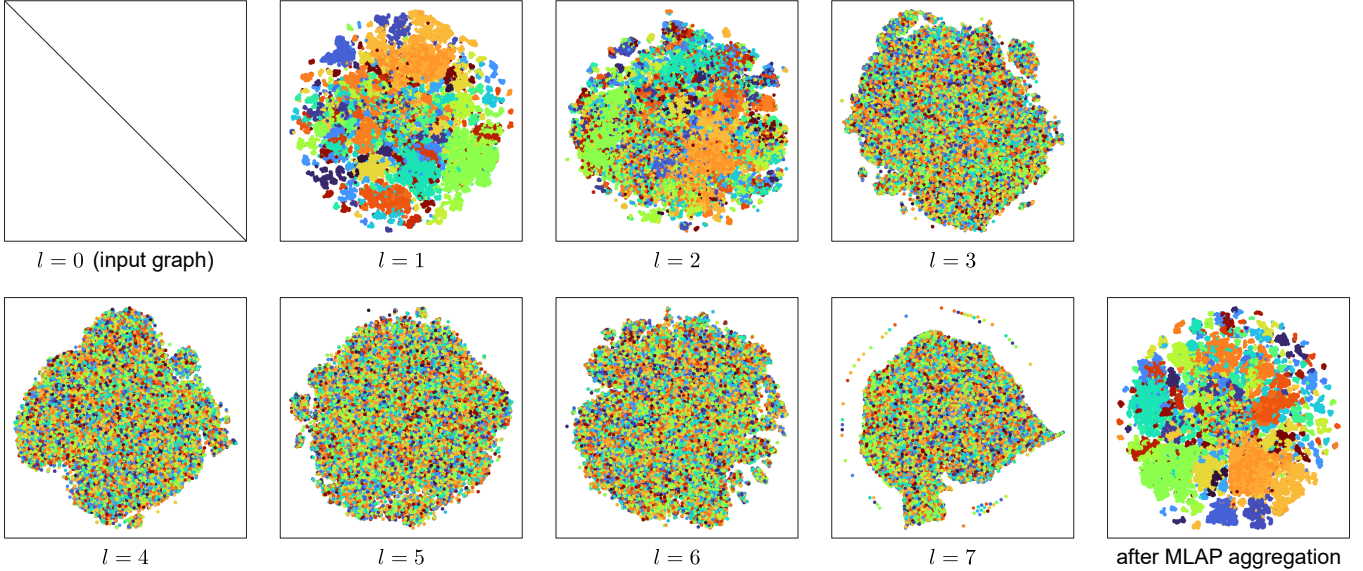


Figure 7: The layer-wise graph representations for ogbg-ppa graphs. They are visualized in two-dimensional spaces using t-SNE. Dots in each color represent samples in a class. Visualization in $l = 0$ is not available because the graphs in the ogbg-ppa dataset do not have initial graph features. (For interpretation of the reference to color in this figure legend, the reader is referred to the web version of this article.)

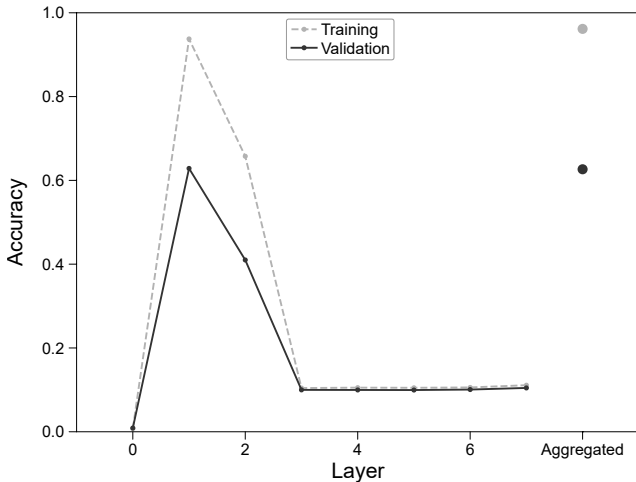


Figure 8: The classification performances of the layer-wise representations computed for ogbg-ppa graphs. The “Aggregated” in the horizontal axis indicates the classifier’s performance trained with the graph representations after MLAP aggregation.

ities in the later layers were low because of oversmoothing. However, in an ogbg-molhiv model, the final graph representation after MLAP aggregation had a better discriminability than any representations in the intermediate layers. These results suggest that the layer-wise graph information in multiple levels of localities contributes complementary to the final graph representation to improve the classification performance of the model. In contrast to the ogbg-molhiv model, the intermediate representations in the ogbg-ppa model had the peak class discriminability just after the first message passing step. This might be because the ogbg-ppa dataset has no initial node features.

We set zero vectors as the initial node representations to initiate message passing among nodes—that is, all nodes had the same initial representations. This situation can be regarded as the node representations were extremely over-smoothed at the beginning of the message passing procedure. Therefore, repeating message passing for multiple steps provided no useful intermediate representations, and hence the aggregated final graph representations were not better than the representation after the first message passing.

Designing neural network architectures by adopting neuroscientific knowledge is a popular research topic. The multi-level attention mechanism introduced in the MLAP architecture can also be seen as an analogy of the attention mechanism in the cognitive system of humans or other primates. Such cognitive system, particularly the visual perception mechanism, is hierarchically organized and accompanied by hierarchical attention mechanisms. For example, the ventral visual pathway contributes to the hierarchical computation of object recognition mechanisms (Kravitz et al., 2013). In the ventral visual pathway, the neural information in the area V1 represents the raw visual inputs, and the representations are hierarchically abstracted towards the inferior temporal cortices as the receptive field—*i.e.*, locality—of the information is expanded. DeWeerd et al. (1999) found that lesions in the cortical areas V4 and TEO, both of which are components in the ventral pathway, contribute to the attentional processing in receptive fields with different sizes. As an example of artificial neural network studies inspired by these neuroscience studies, Taylor et al. (2009) proposed a method to autonomously control a robot using a neural network model with a hierarchical attention system, in

which goal-oriented attention signals mediates the behavior of the network. Brain-inspired neural network architecture would improve the performance or the efficiency of the models, whereas the computational studies on neural networks might contribute back to neuroscience research. Hence, the neuroscience and artificial neural network will keep on affecting mutually and developing along with each other.

There are several possible directions to extend the proposed methods further. First, exploring the form of aggregator functions other than the ones proposed in this study, *i.e.*, *sum* and *weighted*, is needed. For example, it is possible to design an aggregator that models the relationships among layer-wise representations, whereas the proposed aggregators treated the layer-wise representations as individual to each other. Also, one can design an aggregator that only uses the representations in a subset of layers to reduce the computational cost, although the proposed aggregators required the layer-wise representations in all of the GNN layers. Second, multi-stage training of the models with MLAP architecture would be beneficial. Instead of training the entire GNN models with MLAP at once, as we did in this study, one can train the GNN backbone without MLAP first *and then* fine-tune the model with the MLAP. This kind of multi-stage training would stabilize the learning process, particularly when using the MLAP with an aggregator that has many trainable parameters. For example, we can possibly improve the performances of *MLAP-weighted* architecture with $L + 1$ trainable parameters, which were not as good as *MLAP-sum* with no additional parameters. Lastly, our MLAP architecture would be adopted to arbitrary deep learning models, even not limited to GNNs. For example, convolutional neural networks (CNNs) for computer vision would be good candidates. Some CNN studies, such as U-Net (Ronneberger et al., 2015), have already considered the hierarchy of the information processed in the neural networks. Adopting the hierarchical attention mechanism to such models might improve their performance.

In conclusion, we proposed the MLAP architecture for GNN models that aggregates graph representations in multiple levels of localities. The results suggest that the proposed architecture is effective in overcoming the performance degradation in deeper GNN models. In the history of deep learning studies, the performance of neural network models *except for GNNs* has improved by increasing the number of layers because deep models have richer expressivity. Therefore, realizing deep *GNN* models using MLAP would be desirable and may extend the applicability of GNNs.

Conflict of Interest

The authors declare no competing financial interests.

Acknowledgements

We thank Y. Ikutani for his valuable comments. This work was supported by JSPS KAKENHI grant number 16H06569, 18K18108, 18K19821, and JP19J20669.

References

- Ahmed, A., Shervashidze, N., Narayanamurthy, S. M., Josifovski, V., & Smola, A. J. (2013). Distributed large-scale natural graph factorization. In *Proceedings of the 22nd International World Wide Web Conference* (pp. 37–48).
- Ba, L. J., Kiros, J. R., & Hinton, G. E. (2016). Layer normalization. *arXiv preprint, arXiv:1607.06450*.
- Bahdanau, D., Cho, K., & Bengio, Y. (2015). Neural machine translation by jointly learning to align and translate. In *Proceedings of the 3rd International Conference on Learning Representations*.
- Belkin, M., & Niyogi, P. (2001). Laplacian eigenmaps and spectral techniques for embedding and clustering. In *Advances in Neural Information Processing Systems 14* (pp. 585–591).
- Bruna, J., Zaremba, W., Szlam, A., & LeCun, Y. (2014). Spectral networks and locally connected networks on graphs. In *Proceedings of the 2nd International Conference on Learning Representations*.
- Cai, T., Luo, S., Xu, K., He, D., Liu, T., & Wang, L. (2020). Graph-Norm: A principled approach to accelerating graph neural network training. *arXiv preprint, arXiv:2009.03294*.
- Cangea, C., Velickovic, P., Jovanovic, N., Kipf, T., & Liò, P. (2018). Towards sparse hierarchical graph classifiers. *arXiv preprint, arXiv:1811.01287*.
- Chen, M., Wei, Z., Huang, Z., Ding, B., & Li, Y. (2020). Simple and deep graph convolutional networks. In *Proceedings of the 37th International Conference on Machine Learning* (pp. 1725–1735).
- Defferrard, M., Bresson, X., & Vandergheynst, P. (2016). Convolutional neural networks on graphs with fast localized spectral filtering. In *Advances in Neural Information Processing Systems 29* (pp. 3837–3845).
- DeWeerd, P., Peralta, M. R., Desimone, R., & Ungerleider, L. G. (1999). Loss of attentional stimulus selection after extrastriate cortical lesions in macaques. *Nature Neuroscience*, 2, 753–758.
- Duvenaud, D. K., Maclaurin, D., Iparraguirre, J., Bombarell, R., Hirzel, T., Aspuru-Guzik, A., & Adams, R. P. (2015). Convolutional networks on graphs for learning molecular fingerprints. In *Advances in Neural Information Processing Systems 28* (pp. 2224–2232).
- Gao, H., & Ji, S. (2019). Graph U-Nets. In *Proceedings of the 36th International Conference on Machine Learning* (pp. 2083–2092).
- Gilmer, J., Schoenholz, S. S., Riley, P. F., Vinyals, O., & Dahl, G. E. (2017). Neural message passing for quantum chemistry. In *Proceedings of the 34th International Conference on Machine Learning* (pp. 1263–1272).
- Gori, M., Monfardini, G., & Scarselli, F. (2005). A new model for learning in graph domains. In *Proceedings of the IEEE International Conference on Bioinformatics and Biomedicine*.
- Hamilton, W. L. (2020). *Graph Representation Learning*. Morgan and Claypool.
- Hamilton, W. L., Ying, R., & Leskovec, J. (2017a). Representation learning on graphs: Methods and applications. *IEEE Data Engineering Bulletin*, 40, 52–74.
- Hamilton, W. L., Ying, Z., & Leskovec, J. (2017b). Inductive representation learning on large graphs. In *Advances in Neural Information Processing Systems 30* (pp. 1024–1034).
- He, K., Zhang, X., Ren, S., & Sun, J. (2016). Deep residual learning for image recognition. In *Proceedings of the 2016 IEEE Conference on Computer Vision and Pattern Recognition* (pp. 770–778).
- Hu, W., Fey, M., Zitnik, M., Dong, Y., Ren, H., Liu, B., Catasta, M., & Leskovec, J. (2020). Open graph benchmark: Datasets for machine learning on graphs. In *Advances in Neural Information Processing Systems 33* (pp. 22118–22133).

- Huang, W., Rong, Y., Xu, T., Sun, F., & Huang, J. (2020). Tackling over-smoothing for general graph convolutional networks. *arXiv preprint, arXiv:2008.09864*.
- Ioffe, S., & Szegedy, C. (2015). Batch normalization: Accelerating deep network training by reducing internal covariate shift. In *Proceedings of the 32nd International Conference on Machine Learning* (pp. 448–456).
- Kingma, D. P., & Ba, J. (2015). Adam: A method for stochastic optimization. In *Proceedings of the 3rd International Conference on Learning Representations*.
- Kipf, T. N., & Welling, M. (2017). Semi-supervised classification with graph convolutional networks. In *Proceedings of the 5th International Conference on Learning Representations*.
- Kondor, R. I., & Lafferty, J. (2002). Diffusion kernels on graphs and other discrete structures. In *Proceedings of the 19th International Conference on Machine Learning* (pp. 315–322).
- Kravitz, D. J., Saleem, K. S., Baker, C. I., Ungerleider, L. G., & Mishkin, M. (2013). The ventral visual pathway: an expanded neural framework for the processing of object quality. *Trends in Cognitive Sciences*, 17, 26–49.
- Lee, J., Lee, I., & Kang, J. (2019). Self-attention graph pooling. In *Proceedings of the 36th International Conference on Machine Learning* (pp. 3734–3743).
- Li, G., Müller, M., Thabet, A. K., & Ghanem, B. (2019). DeepGCNs: Can GCNs go as deep as CNNs? In *Proceedings of the 2019 IEEE/CVF International Conference on Computer Vision* (pp. 9266–9275).
- Li, Q., Han, Z., & Wu, X. (2018). Deeper insights into graph convolutional networks for semi-supervised learning. In *Proceedings of the 32nd AAAI Conference on Artificial Intelligence* (pp. 3538–3545).
- Li, Y., Tarlow, D., Brockschmidt, M., & Zemel, R. S. (2016). Gated graph sequence neural networks. In *Proceedings of the 4th International Conference on Learning Representations*.
- van der Maaten, L., & Hinton, G. (2008). Visualizing data using t-SNE. *Journal of Machine Learning Research*, 9, 2579–2605.
- Niepert, M., Ahmed, M., & Kutzkov, K. (2016). Learning convolutional neural networks for graphs. In *Proceedings of the 33rd International Conference on Machine Learning* (pp. 2014–2023).
- Page, L., Brin, S., Motwani, R., & Winograd, T. (1999). *The PageRank Citation Ranking: Bringing Order to the Web*. Technical Report 1999-66 Stanford InfoLab.
- Ronneberger, O., Fischer, P., & Brox, T. (2015). U-Net: Convolutional networks for biomedical image segmentation. In *Proceedings of the International Conference on Medical Image Computing and Computer-Assisted Intervention* (pp. 234–241).
- Scarselli, F., Gori, M., Tsoi, A. C., Hagenbuchner, M., & Monfardini, G. (2009). The graph neural network model. *IEEE Transactions on Neural Networks*, 20, 61–80.
- Shervashidze, N., Schweitzer, P., van Leeuwen, E. J., Mehlhorn, K., & Borgwardt, K. M. (2011). Weisfeiler-Lehman graph kernels. *Journal of Machine Learning Research*, 12, 2539–2561.
- Szklarczyk, D., Gable, A. L., Lyon, D., Junge, A., Wyder, S., Huerta-Cepas, J., Simonovic, M., Doncheva, N. T., Morris, J. H., Bork, P., Jensen, L. J., & Mering, C. (2018). STRING v11: protein–protein association networks with increased coverage, supporting functional discovery in genome-wide experimental datasets. *Nucleic Acids Research*, 47, D607–D613.
- Taylor, J. G., Hartley, M., Taylor, N., Panchev, C., & Kasderidis, S. (2009). A hierarchical attention-based neural network architecture, based on human brain guidance, for perception, conceptualisation, action and reasoning. *Image and Vision Computing*, 27, 1641–1657.
- Ulyanov, D., Vedaldi, A., & Lempitsky, V. S. (2016). Instance normalization: The missing ingredient for fast stylization. corr abs/1607.08022 (2016). *arXiv preprint, arXiv:1607.08022*.
- Veličković, P., Cucurull, G., Casanova, A., Romero, A., Liò, P., & Bengio, Y. (2018). Graph attention networks. In *Proceedings of the 6th International Conference on Learning Representations*.
- Vinyals, O., Bengio, S., & Kudlur, M. (2016). Order matters: Sequence to sequence for sets. In *Proceedings of the 4th International Conference on Learning Representations*.
- Wu, Z., Pan, S., Chen, F., Long, G., Zhang, C., & Yu, P. S. (2021). A comprehensive survey on graph neural networks. *IEEE Transactions on Neural Networks and Learning Systems*, 32, 4–24.
- Wu, Z., Ramsundar, B., Feinberg, E. N., Gomes, J., Geniesse, C., Pappu, A. S., Leswing, K., & Pande, V. (2018). MoleculeNet: a benchmark for molecular machine learning. *Chemical Science*, 9, 513–530.
- Xu, K., Hu, W., Leskovec, J., & Jegelka, S. (2019). How powerful are graph neural networks? In *Proceedings of the 7th International Conference on Learning Representations*.
- Xu, K., Li, C., Tian, Y., Sonobe, T., Kawarabayashi, K., & Jegelka, S. (2018). Representation learning on graphs with jumping knowledge networks. In *Proceedings of the 35th International Conference on Machine Learning* (pp. 5453–5462). volume 80.
- Ying, Z., You, J., Morris, C., Xiang, R., Hamilton, W. L., & Leskovec, J. (2018). Hierarchical graph representation learning with differentiable pooling. In *Advances in Neural Information Processing Systems 31* (pp. 4805–4815).
- Zhang, J., & Meng, L. (2019). GResNet: Graph residual network for reviving deep gnn from suspended animation. *arXiv preprint, arXiv:1909.05729*.
- Zhang, M., Cui, Z., Neumann, M., & Chen, Y. (2018a). An end-to-end deep learning architecture for graph classification. In *Proceedings of the 32nd AAAI Conference on Artificial Intelligence* (pp. 4438–4445).
- Zhang, Z., Cui, P., & Zhu, W. (2018b). Deep learning on graphs: A survey. *arXiv preprint, arXiv:1812.04202*.
- Zhao, L., & Akoglu, L. (2020). PairNorm: Tackling oversmoothing in gnns. In *Proceedings of the 8th International Conference on Learning Representations*.